ORIGINAL PAPER

Wellbore collapse caused by thermo-chemical coupling effects drilling in shale formation

Hu Yin[1] · Zhiqiang Tang[2] · Liming Dai[3] · Hao Peng[4]

Abstract
Wellbore instability in shale formations has always been a concern in oil exploration field. According to the Mohr–Coulomb criterion, a new model for evaluating and classifying the collapse of horizontal wellbore in shale formation is established. In this model, the temperature field and the pore pressure field affected by hydraulic pressure, thermal potential, and chemical potential difference between the drilling fluid and formation fluid are considered. Using the model, the influences of the temperature and solute concentration of drilling fluid on the failure degree of horizontal wellbore in shale formation with weak planes are simulated and analyzed. Based on the research results, weak planes that exist in shale formation will cause a significant wellbore collapse and using cool drilling fluid with high solute concentration can reduce the collapse degree of horizontal wellbore. The model established may help drilling engineers in practice to take effective measures for reducing wellbore instability and avoiding possible wellbore collapse during drilling in shale formations.

Keywords Shale formation · Wellbore collapse · Thermo-chemical coupling · Weak plane · Shale formation · Horizontal well

Introduction

It is almost inevitable that a drilling process will encounter a shale formation, because shale formations are ubiquitous in sedimentary basins worldwide (Speight 2016). With the great success of shale oil and gas exploration, wellbore stability of shale formation has been an important research area within drilling engineering in recent years. Shale rock contains many weak planes that will cause shale rock failure under a lower stress conditions (Ding et al. 2018). As to the effects of weak planes on the strength of material such as shale, Jaeger (1960) used two Mohr–Coulomb envelopes to describe the failure of the material itself and the failure along weak planes respectively. Since then, many authors have considered failure along the weak plane in their research on the wellbore stability of shale formations (Aadnoy and Chenevert 1987; Narayanasamy et al. 2010; Lee et al. 2012; Liang et al. 2014; He et al. 2015; Ma and Chen 2015; Gao et al. 2017a, b; Ding et al. 2018; Zhou et al. 2018). In addition, the variation of pore pressure and temperature around the wellbore may also have a great influence on wellbore stability during drilling shale formations (Mody and Hale 1993; Wang and Papamichos 1994; Chen et al. 2003; Rahman et al. 2003; Chen and Ewy 2005; Ghassemi et al. 2009). Mody and Hale (1993) confirmed that hydraulic pressure and chemical potential of drilling fluid will change the pore pressure near the wellbore. Both Chen and Ewy (2005) and Ghassemi et al. (2009) established thermo-chemical coupling models and analyzed the effects of drilling fluid solute concentration and temperature on the stress distribution around the wellbore in shale formation. Ma and Chen (2015) established a model that considers the influence of drilling fluid solute concentration and weak planes on wellbore stability of shale formation, but neglected the temperature changes.

✉ Zhiqiang Tang
tangzhiqiangb523@163.com

1 Petroleum Engineering School, Southwest Petroleum University, Chengdu 610500, Sichuan, China

2 Guang'an Vocational & Technical College, Guang'an, Sichuan 638500, China

3 Industrial Systems Engineering, University of Regina, Regina, SK S4S0A2, Canada

4 CNPC Chuanqing Drilling Engineering Company Limited Chuanxi Drilling Company, Chengdu 610500, Sichuan, China

The influence of temperature difference on wellbore failure can be significant because temperature diffusion is much faster than solute and hydraulic diffusions in shale rock. Gao et al. (2017a, b) simulated the effects of temperature and weak shale on formation wellbore failure, but neglected the influence of solute concentration, which is not negligible during drilling a shale formation. Drilling a shale formation, both the weak planes existing in shale formation and the drilling fluid performance, including the temperature and the solute concentration, has a significant influence on wellbore stability.

In order to accurately predict the wellbore stability of shale formation, this paper will present a new model that will consider the effects of both weak planes and drilling fluid performance. Using this new model, the influence of the weak planes and the temperature and solute concentration of drilling fluid on the failure degree of wellbore of shale formation will be simulated.

Stresses acting on the near-wellbore rock

Shale rock is generally considered as an anisotropic material with transversely isotropic properties (Li and Weijermars 2019; Wang et al. 2020; Dubey et al. 2021). Jin et al. (2012) analyzed the effect of this property of shale rock on the stress distribution and showed that the effect is relatively small. Therefore, Ma and Chen (2015) ignored this effect in the process of deriving the wellbore stress distribution. Usually, the stress distribution of wellbore is considered a time-independent function of in situ stress, wellbore orientation, wellbore pressure, and pore pressure, given by the well-known Kirsch equation (Bradley 1979; Lee et al. 2012). However, because there are more or less difference between the drilling fluid and the formation liquid in temperature, pressure, and solute concentration, both the pore pressure and the formation temperature near the wellbore will change with time, altering the stress distribution around the wellbore. Assuming the variation of pore pressure and formation temperature with time is axisymmetric, Tang et al. (2018) derived the instantaneous stress distribution around the horizontal wellbore, as shown in Eq. (1).

$$
\begin{cases}
\sigma_{rr} = \frac{\sigma_{11}+\sigma_{22}}{2}(1 - \frac{r_w^2}{r^2}) + \frac{\sigma_{11}-\sigma_{22}}{2}(1 + 3\frac{r_w^4}{r^4} - 4\frac{r_w^2}{r^2})\cos 2\theta \\
\quad + \sigma_{12}(1 + 3\frac{r_w^4}{r^4} - 4\frac{r_w^2}{r^2})\sin 2\theta + \frac{r_w^2}{r^2}P_w + \sigma_{rr,pore} + \sigma_{rr,thero} \\
\sigma_{\theta\theta} = \frac{\sigma_{11}+\sigma_{22}}{2}(1 + \frac{r_w^2}{r^2}) - \frac{\sigma_{11}-\sigma_{22}}{2}(1 + 3\frac{r_w^4}{r^4})\cos 2\theta \\
\quad - \sigma_{12}(1 + 3\frac{r_w^4}{r^4})\sin 2\theta - \frac{r_w^2}{r^2}P_w + \sigma_{\theta\theta,pore} + \sigma_{\theta\theta,thero} \\
\sigma_{zz} = \sigma_{33} - 2\nu(\sigma_{11} - \sigma_{22})\frac{r_w^2}{r^2}\cos 2\theta - 4\nu\sigma_{12}\frac{r_w^2}{r^2}\sin 2\theta + \sigma_{zz,pore} \\
\quad + \sigma_{zz,thero} \tau_{r\theta} = (\frac{\sigma_{22}-\sigma_{11}}{2}\sin 2\theta + \sigma_{12}\cos 2\theta)(1 + \frac{2r_w^2}{r^2} - 3\frac{r_w^4}{r^4}) \\
\tau_{rz} = (\sigma_{23}\sin\theta + \sigma_{13}\cos\theta)(1 - \frac{r_w^2}{r^2})\tau_{\theta z} = (\sigma_{23}\cos\theta - \sigma_{13}\sin\theta)(1 + \frac{r_w^2}{r^2})
\end{cases}
\tag{1}
$$

where θ is the well round angle, r_w is the wellbore radius, r is the radial distance from wellbore axis, P_w is the internal wellbore pressure, and ν is the Poisson's ratio. The stresses caused by pore pressure and temperature changes are given by (Chen et al. 2003; Wang and Papamichos 1994):

$$
\begin{cases}
\sigma_{rr,pore} = \frac{\eta(1-2\nu)}{(1-\nu)r^2}\int_{r_w}^{r}[P(\rho,t) - P_0]\rho d\rho - \eta P(r,t) \\
\sigma_{\theta\theta,pore} = -\frac{\eta(1-2\nu)}{(1-\nu)}\{\frac{1}{r^2}\int_{r_w}^{r}[P(\rho,t) - P_0]\rho d\rho - [P(r,t) - P_0]\} - \eta P(r,t) \\
\sigma_{zz,pore} = \frac{\eta(1-2\nu)}{1-\nu}[P(r,t) - P_0] - \eta P(r,t)
\end{cases}
\tag{2}
$$

$$
\begin{cases}
\sigma_{rr,thero} = \frac{E\alpha_m^T}{3(1-\nu)r^2}\int_{r_w}^{r}[T(\rho,t) - T_0]\rho d\rho \\
\sigma_{\theta\theta,thero} = -\frac{E\alpha_m^T}{3(1-\nu)}\{\frac{1}{r^2}\int_{r_w}^{r}[T(\rho,t) - T_0]\rho d\rho - [T(r,t) - T_0]\} \\
\sigma_{zz,thero} = \frac{E\alpha_m^T}{3(1-\nu)}[T(r,t) - T_0]
\end{cases}
\tag{3}
$$

where P_0 is the initial pore pressure, E is the Young's modulus, α_m^T is the thermal expansion coefficient of rock, T_0 is the initial formation temperature, t is the time, η is the Biot's coefficient, and $T(r,t)$ and $P(r,t)$ are the instantaneous temperature field and the pore pressure field respectively. The mathematical description of the temperature field is shown in the Appendix.

In Eq. (1), $\sigma_{ij}(i,j = 1, 2, 3)$ is the stress components of in situ stress in the Cartesian coordinate system of wellbore, given by Eq. (4).

$$
\begin{cases}
\sigma_{11} = \cos^2\beta[S_H\cos^2(\alpha - \alpha_H) + S_h\sin^2(\alpha - \alpha_H)] + S_V\sin^2\beta \\
\sigma_{22} = S_H\sin^2(\alpha - \alpha_H) + S_h\cos^2(\alpha - \alpha_H) \\
\sigma_{33} = \sin^2\beta[S_H\cos^2(\alpha - \alpha_H) + S_h\sin^2(\alpha - \alpha_H)] + S_V\cos^2\beta \\
\sigma_{12} = (S_h - S_H)\cos\beta\cos(\alpha - \alpha_H)\sin(\alpha - \alpha_H) \\
\sigma_{13} = [S_H\cos^2(\alpha - \alpha_H) + S_h\sin^2(\alpha - \alpha_H) - S_V]\sin\beta\cos\beta \\
\sigma_{23} = (S_h - S_H)\sin\beta\cos(\alpha - \alpha_H)\sin(\alpha - \alpha_H)
\end{cases}
\tag{4}
$$

where S_H is the maximum horizontal stress, S_h is the minimum horizontal stress, S_V is the vertical stress, α_H is the maximum horizontal stress direction angle from the north direction, α is the wellbore azimuth angle from the north direction, and β is the wellbore inclination angle.

When the failure across intact rock around the wellbore occurs, the radial stress σ_{rr} is one of the three principal stresses acting on the rock, and the other two principal stresses (σ_{tmax} and σ_{tmin}) are as follows (Peška and Zoback 1995; Zoback et al. 2003):

$$
\begin{cases}
\sigma_{tmax} = \frac{1}{2}[\sigma_{zz} + \sigma_{\theta\theta} + \sqrt{(\sigma_{zz} - \sigma_{\theta\theta})^2 + 4\tau_{\theta z}^2}] \\
\sigma_{tmin} = \frac{1}{2}[\sigma_{zz} + \sigma_{\theta\theta} - \sqrt{(\sigma_{zz} - \sigma_{\theta\theta})^2 + 4\tau_{\theta z}^2}]
\end{cases}
\tag{5}
$$

Stresses acting on weak planes

The principal stresses acting on the tangent plane of well-bore wall $\sigma_{t\max}$, $\sigma_{t\min}$, and σ_{rr} in Eq. (5) are in the Cartesian coordinate system. Because the parameters of this Cartesian coordinate system are unknown, it is difficult to convert these three principal stresses to the weak plane. Since knowing the stress components in the wellbore cylinder coordinate system Eq. (1), we can convert the stress components to the wellbore Cartesian coordinate system. Figure 1 shows the conversion relationship between the two coordinate systems.

The coordinate transformation matrix between Cartesian and cylindrical coordinate systems is given by:

$$C = \begin{bmatrix} \cos\theta & \sin\theta & 0 \\ -\sin\theta & \cos\theta & 0 \\ 0 & 0 & 1 \end{bmatrix} \tag{6}$$

Set up a global coordinate system $O\text{-}XYZ$, in which the $O\text{-}X$ axis points to true north and $O\text{-}Y$ axis points to true East. Rotating the $O\text{-}Z$ axis with a rotation angle equaling to wellbore azimuth angle (α) and rotating the $O\text{-}Y$ axis with a rotation angle equaling to wellbore inclination angle (β), the Cartesian coordinate system of wellbore ($o - x_b y_b z_b$) can be obtained, as shown in Fig. 2. Therefore, the conversion matrix between global and wellbore coordinate systems is given by Eq. (7).
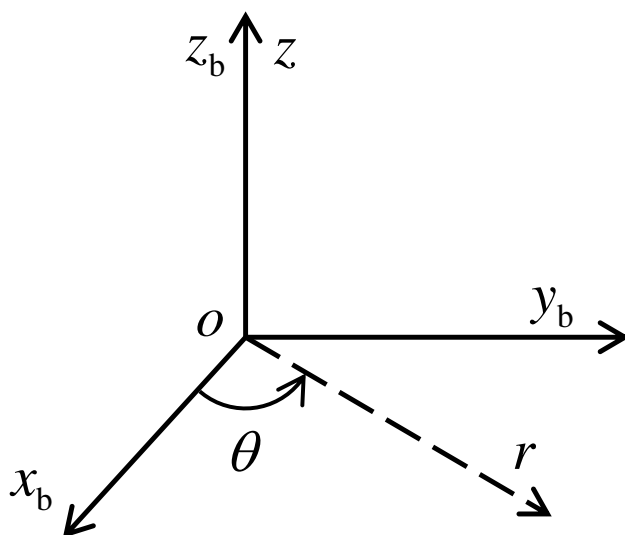
$$B = \begin{bmatrix} \cos\beta & 0 & -\sin\beta \\ 0 & 1 & 0 \\ \sin\beta & 0 & \cos\beta \end{bmatrix} \begin{bmatrix} \cos\alpha & \sin\alpha & 0 \\ -\sin\alpha & \cos\alpha & 0 \\ 0 & 0 & 1 \end{bmatrix}$$
$$= \begin{bmatrix} \cos\alpha\cos\beta & \sin\alpha\cos\beta & -\sin\beta \\ -\sin\alpha & \cos\alpha & 0 \\ \cos\alpha\sin\beta & \sin\alpha\sin\beta & \cos\beta \end{bmatrix} \tag{7}$$

Similarly, rotating the $O\text{-}Z$ axis with a rotation angle equaling to the dip direction of weak plane (α_w) and rotating the $O\text{-}Y$ axis with a rotation angle equaling to dip angle of weak plane (β_w), the Cartesian coordinate system of weak plane ($o - x_w y_w z_w$) can be obtained, as shown in Fig. 3.

The conversion matrix between global and weak plane coordinate systems is given by Eq. (8).

$$\begin{bmatrix} \cos\alpha_w\cos\beta_w & \sin\alpha_w\cos\beta_w & -\sin\beta_w \\ -\sin\alpha_w & \cos\alpha_w & 0 \\ \cos\alpha_w\sin\beta_w & \sin\alpha_w\sin\beta_w & \cos\beta_w \end{bmatrix} \tag{8}$$

Lee et al. (2012) put forward the process that how to convert the stress distribution from wellbore cylindrical coordinate system (σ_{CCS}) to the Cartesian coordinate system of weak plane, given by:

$$\begin{bmatrix} \sigma_{xx}^w & \tau_{xy}^w & \tau_{xz}^w \\ \tau_{xy}^w & \sigma_{yy}^w & \sigma_{yy}^w \\ \tau_{xz}^w & \tau_{yz}^w & \sigma_{zz}^w \end{bmatrix} = WB^T C^T \sigma_{CCS} C B W^T \tag{9}$$
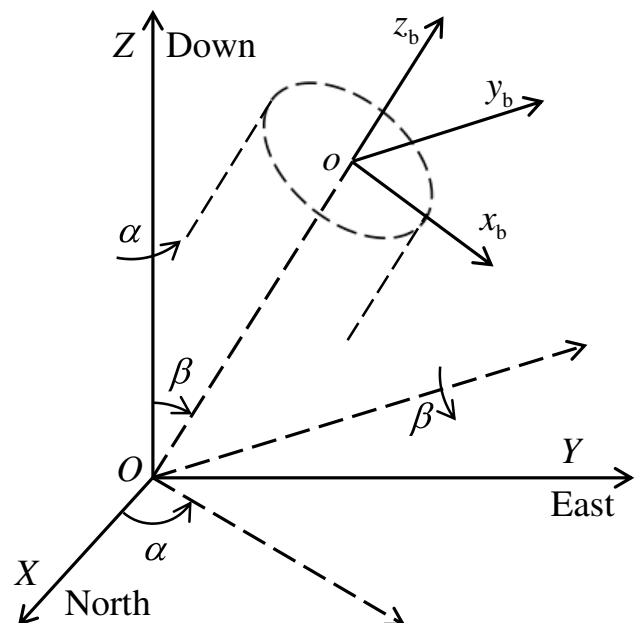

Fig. 1 Conversion relationship between Cartesian and cylindrical coordinate systems

Fig. 2 Conversion relationship between global and wellbore coordinate systems

Fig. 3 Conversion relationship between global and weak plane coordinate systems

Fig. 4 The stresses acting on the weak plane

where $\sigma_{\text{CCS}} = \{\sigma_{rr}, \tau_{r\theta}, \tau_{rz}; \tau_{r\theta}, \sigma_{\theta\theta}, \tau_{\theta z}; \tau_{r\theta}, \tau_{\theta z}, \sigma_{zz}\}$ is the stress distribution in wellbore cylindrical coordinate system, given by Eq. (1).

Then, we can obtain the normal stress (σ_n) and shear stress (τ) acting on the plane of weakness (Fig. 4), given by:

$$\begin{cases} \sigma_n = \sigma_{zz}^w \\ \tau = \sqrt{(\tau_{zx}^w)^2 + (\tau_{zy}^w)^2} \end{cases} \tag{10}$$

Wellbore failure of shale formation

Once the stress distribution around wellbore has been obtained, whether wellbore will fail and the failure degree of wellbore can be determined by using the rock failure criterion. Unlike conventional formations, shear failures of wellbore in shale formations include the failure of rock body and the failure along weak planes. Since the strength (cohesion and internal friction angle) of weak plane is much lower than that of rock body, even a low shear stress can easily cause the sliding of weak plane. Jaeger (1960) used the Mohr–Coulomb criterion to analyze the failure of material containing weak planes. For the failure across intact rock, we can use the Mohr–Coulomb criterion presented in terms of principal stress (Jaeger et al. 2009):
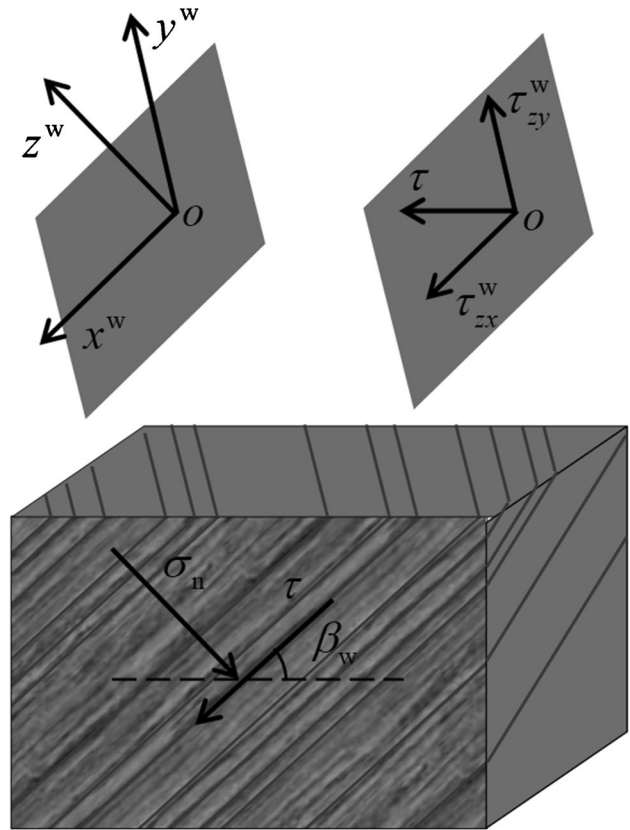
$$\sigma_1 = UCS + \sigma_3 \tan^2(45° + \varphi/2) \tag{11}$$

where σ_1 and σ_3 are major and minor effective principal stress respectively, UCS is the uniaxial compressive strength of rock, and φ is the internal friction angle of rock.

Shear failure of wellbore is usually due to a low wellbore pressure. Therefore, if shear failure occurs on the wellbore wall, the effective stresses are usually as follows:

$$\sigma_1 = \sigma_{t\max}; \sigma_3 = \sigma_{rr} \tag{12}$$

Substituting the normal stress and shear stress acting on the plane of weakness (Eq. 10) into the Mohr–Coulomb criterion presented in terms of shear stress, we can obtain the following equation:

$$\tau = S_w + \sigma_n \tan\varphi_w \tag{13}$$

where S_w is the cohesion of weak plane and φ_w is internal friction angle of weak plane.

Using Eq. (11) to Eq. (13), we can calculate the values of r at the point where the failure of rock and weak planes occurs in all directions around the wellbore, and then determine the degree of wellbore failure.

Example for analysis

In order to study the effects of drilling fluid performance and weak plane on the stability of wellbore in shale formation, we assume a horizontal wellbore of shale formation and the relevant data, including parameters of rock mechanics and parameters of drilling fluid performance, are given in Table 1.

Using these parameters and the rock failure criterion, we can determine the shear failure radius of the wellbore in all directions. Through the C# program, we can simulate and draw the area of wellbore failure and intuitively understand the failure degree of wellbore in shale rock. The failures of wellbore under different drilling conditions are shown in Figs. 5, 6, and 7. The blue lines show the area of failure across intact rock around the wellbore and the red lines show the area of failure along weak planes. Compared to the two conventional shear failures

that symmetrically occur on the wellbore wall, the sliding of the weak planes will cause four failures, symmetrically appearing on the wellbore wall.

Assuming that $T_w = 300K, T_0 = 350K, C_w = 0.25, C_0 = 0.05$, the wellbore failures at 2 h, 5 h, and 10 h are simulated as shown in Fig. 5. When the solute concentration of drilling fluid is greater than that of formation fluid, the degree of wellbore failure is relatively small. The results show the wellbore expansion is mainly caused by the failure of weak plane, and the wellbore expansion caused by the failure of rock body is not obvious. The shear failure occurs near the upper and lower parts of the wellbore cross-section, and the maximum diameter expansion direction is about 40° away from the vertical axis. As the time increases, the degree of wellbore expansion will first decrease and then increase, but the change is not obvious. The maximum expansion rates of the wellbore are 8.95%, 6.74%, and 8.81%, respectively.

Table 1 Parameters for analysis (Tang et al. 2018; Ghassemi et al. 2009)

| Parameters	Values	Units	Parameters	Values	Units
Wellbore radius r_w	0.108	m	Fluid density ρ_f	1111.1	kg·m^{-3}
Initial pore pressure P_0	20	MPa	Solute molar mass M^S	0.0585	kg·mol^{-1}
Wellbore pressure P_w	30	MPa	Thermal osmotic coefficient K^T	6.0e^{-11}	m^2·s^{-1}·K^{-1}
Uniaxial compressive strength UCS	47	MPa	Thermal diffusivity c^T	1.6e^{-6}	m^2·s^{-1}
Poisson's ratio ν	0.22	/	Solute diffusivity D^S	2.0e^{-9}	m^2·s^{-1}
Internal friction angle φ	34.2	deg	Thermal diffusion coefficient D^T	6.0e^{-12}	m^2·s^{-1} K^{-1}
Porosity ϕ	0.05	/	Chemical swelling coefficient ω	1.5	MPa
Cohesion of weak plane S_w	5.7	MPa	Inclination angle β	45	deg
Internal friction angle of weak plane φ_w	26.5	deg	Rock bulk modulus K	10,133	MPa
Dip direction of weak plane α_w	30	deg	Rock shear modulus G	6977	MPa
Dip angle of weak plane β_w	45	deg	Reflection coefficient $\mathfrak{R}$	0.2	/
Maximum horizontal stress direction α_H	90	deg	Thermal expansion coefficient of rock matrix α_m^T	1.8e^{-5}	K^{-1}
Minimum horizontal stress S_h	40.6	MPa	Thermal expansion coefficient of fluid α_f^T	3.0e^{-4}	K^{-1}
Maximum horizontal stress S_H	61.3	MPa	Permeability coefficient κ	3.33e^{-16}	m^2·Pa^{-1}·s^{-1}
Vertical stress S_V	45.2	MPa	Biot's coefficient η	0.689	/
Wellbore azimuth angle α	30	deg	Skempton coefficient B	0.824	/

Fig. 5 The wellbore failure at high drilling fluid concentrations

(2 hr)   (5 hr)   (10 hr)
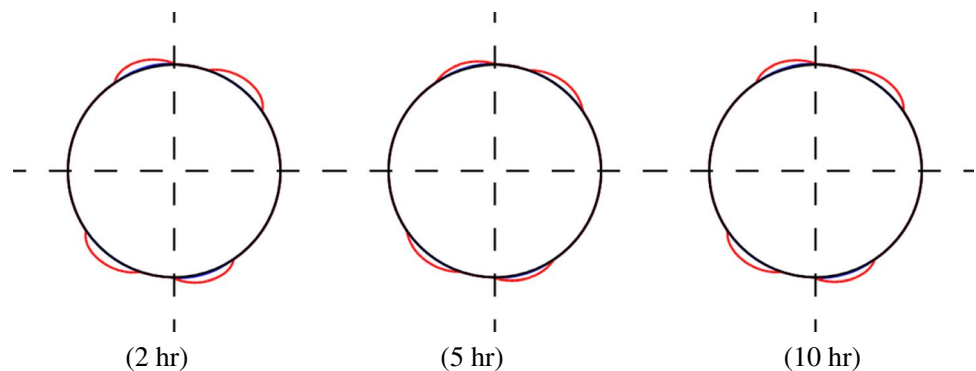
Fig. 6 The wellbore failure at high drilling fluid concentrations and temperature

(2 hr)   (5 hr)   (10 hr)
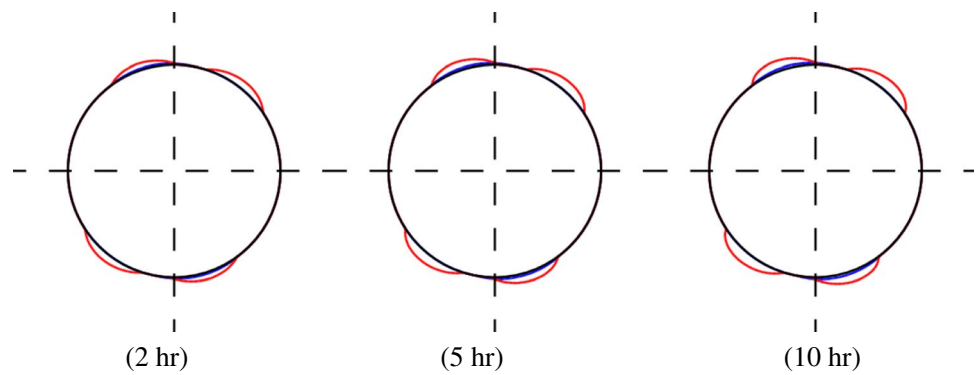
Fig. 7 The wellbore failure at low drilling fluid concentrations

(2 hr)   (5 hr)   (10 hr)
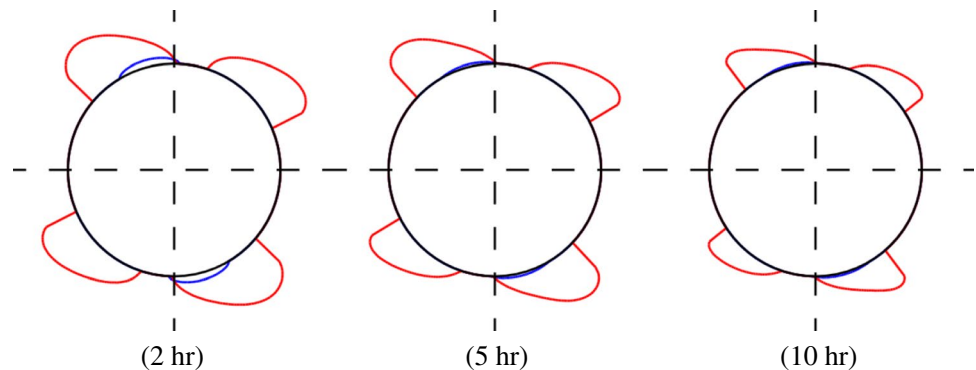
If that $T_w = 350K$, $T_0 = 350K$, $C_w = 0.25$, $C_0 = 0.05$, the wellbore failures at 2 h, 5 h, and 10 h are shown as in Fig. 6. Compared to Fig. 5, increasing the drilling fluid temperature will slightly increase the wellbore failure, including conventional wellbore failure and failure along weak plane. The maximum expansion rates of the wellbore are 7.25%, 9.85%, and 10.88%, respectively. Therefore, the cooling effect of drilling fluid will be constructive to the stability of horizontal wellbore in shale formation. When conditions permit, a drilling fluid cooling device should be added to the wellhead to cool the circulating hot drilling fluid.

Figure 7 shows the failure degree of wellbore drilled for 2 h, 5 h, and 10 h, and the temperature and solute concentration are $T_w = 300K$, $T_0 = 350K$, $C_w = 0.05$, $C_0 = 0.25$. The comparison of Figs. 5 and 7 indicates that the wellbore will experience a significant failure especially failure along weak plane if the solute concentration of drilling fluid is less than formation fluid. The maximum expansion rates of the wellbore are 44.67%, 41.33%, and 31.21%, respectively. Although the figures show that the failure degree will decrease with time, it is meaningless once a significant failure occurs. Therefore, drilling fluid with a high solute concentration is more important for the wellbore stability during drilling a shale formation.

Conclusion

It is found in this research that the failure degree of a horizontal wellbore in shale formation is significantly affected by drilling fluid performance and drilling operation, in addition to the effects of wellbore pressure and drilling direction. The wellbore failure in shale formation may be deteriorated under the coupling effects of hydraulic, chemical, and thermal potential gradients between the drilling fluid and formation fluid. A model is established in this research for analyzing the wellbore failure during drilling processes in shale formations. The model shows efficiency in analyzing the effects of pore pressure changes, temperature, and stress on wellbore failure in shale formation with weak planes. It is found in the research that the presence of weak planes, such as stratum bedding plane existing in shale formations, may have a significant impact on wellborn failure. Also, a low solute concentration of drilling fluid may cause a serious wellbore failure, especially the failure along the weak plane, when drilling a shale formation. Additionally, the cooling effect of drilling fluid can be constructive to the stability of horizontal wellbore in shale formation. Based on the research results, some effective measures can be developed to improve wellbore stability in the operation practices.

Appendix

The temperature field around a wellbore can be expressed as (Tang et al. 2018)

$$T(r,t) - T_0 = \frac{(T_w - T_0)Ei(-u(r,t))}{Ei(-u(r_w,t))} \tag{A1}$$

where

$$Ei(-x) = \gamma + \ln x + \sum_{k=1}^{\infty} \frac{(-1)^k x^k}{k!k} \tag{A2}$$

$$u(r,t) = \frac{r^2}{4c^T t} \tag{A3}$$

and γ is the Euler constant, $\gamma \approx 0.5772$; c^T is the thermal diffusivity.

Tang et al. (2018) also presented an analytic expression to calculate the pore pressure considering the thermo-chemical coupling effect, given by

$$P(r,t) = K^P \frac{Ei(-f(r,t))}{Ei(-f(r_w,t))} + K^{TP} \frac{Ei(-u(r,t))}{Ei(-u(r_w,t))} + K^{CP} \frac{Ei(-g(r,t))}{Ei(-g(r_w,t))} + P_0 \tag{A4}$$

where

$$f(r,t) = \frac{r^2}{4C^F t} \tag{A5}$$

$$g(r,t) = \frac{\phi r^2}{4D^S t} \tag{A6}$$

$$K^P = P_w - P_0 - \frac{D^S C^{CF}}{D^S - \phi C^F}(C_w - C_0) \\ -[\frac{c^T C^{TF}}{c^T - C^F} + (\frac{c^T C^{CF}}{c^T - C^F} - \frac{D^S C^{CF}}{D^S - \phi C^F})\frac{\overline{C}^S D^T}{c^T \phi - D^S}](T_w - T_0) \tag{A7}$$

$$K^{TP} = (\frac{c^T C^{TF}}{c^T - C^F} + \frac{c^T C^{CF}}{c^T - C^F}\frac{\overline{C}^S D^T}{c^T \phi - D^S})(T_w - T_0) \tag{A8}$$

$$K^{CP} = \frac{D^S C^{CF}}{D^S - \phi C^F}[C_w - C_0 - \frac{\overline{C}^S D^T}{c^T \phi - D^S}(T_w - T_0)] \tag{A9}$$

$$C^F = \kappa \frac{3BK(1-\nu)}{3\eta(1-\nu) - 2B\eta^2(1-2\nu)} \tag{A10}$$

$$C^{CF} = -C^F[\frac{\Re \rho_f R \overline{T}}{M^S \overline{C}^S(1-\overline{C}^S)}\frac{\phi}{D^S} - \frac{1}{\kappa}\frac{\eta\omega(1-2\nu)}{2G(1-\nu)}] \tag{A11}$$

$$C^{TF} = \frac{C^F}{\kappa}[\kappa\frac{\Re \rho_f R \overline{T}}{M^S(1-\overline{C}^S)}\frac{D^T}{D^S c^T} - \frac{\eta(1+\nu)}{3(1-\nu)}\alpha_m^T + (\eta\alpha_m^T - \phi\alpha_m^T + \phi\alpha_f^T) + \frac{K^T}{c^T}] \tag{A12}$$

In Eq. (A5) to Eq. (A12), ϕ is the porosity, D^S is the solute diffusivity, C_0 is the solute mass fraction of formation fluid, C_w is the solute mass fraction of drilling fluid, $\overline{C}^S$ is the mean solute mass faction of drilling and formation fluids, D^T is the thermal diffusion coefficient, G is the shear modulus of rock, K is the bulk modulus of rock, ρ_f is the fluid density, ω is the chemical swelling coefficient, B is the Skempton coefficient, T_w is the temperature of drilling fluid, $\overline{T}$ is the mean temperature of drilling fluid and formation, κ is the permeability coefficient of rock, $\Re$ is the reflection coefficient, M^S is the solute molar mass, R is the ideal gas constant, α_f^T is the thermal expansion coefficient of fluid, α_m^T is the thermal expansion coefficient of rock matrix, and K^T is the thermal osmotic coefficient.

Declarations

Conflict of interest The authors declare that they have no competing interests.

References

Aadnoy BS, Chenevert ME (1987) Stability of highly inclined boreholes. SPE Drill Eng 2(4):364–374

Bradley WB (1979) Failure of inclined boreholes. J Energy Res Technol 101(4):232–239

Chen G, Chenevert ME, Sharma MM, Yu M (2003) A study of wellbore stability in shales including poroelastic, chemical, and thermal effects. J Petrol Sci Eng 38(3):167–176

Chen G, Ewy RT (2005) Thermoporoelastic effect on wellbore stability. SPE J 10(02):121–129

Ding Y, Luo P, Liu X, Liang L (2018) Wellbore stability model for horizontal wells in shale formations with multiple planes of weakness. J Nat Gas Sci Eng 52:334–347

Dubey V, Abedi S, Noshadravan A (2021) A multiscale modeling of failure accumulation and permeability variation in shale rocks under mechanical loading. J Petrol Sci Eng 198:108123

Gao J, Deng J, Lan K, Song Z, Feng Y, Chang L (2017a) A poro-thermoelastic solution for the inclined borehole in a transversely isotropic medium subjected to thermal osmosis and thermal filtration effects. Geothermics 67:114–134

Gao J, Deng J, Lan K, Feng Y, Zhang W, Wang H (2017b) Porothermoelastic effect on wellbore stability in transversely isotropic medium subjected to local thermal non-equilibrium. Int J Rock Mech Min Sci 96:66–84

Ghassemi A, Tao Q, Diek A (2009) Influence of coupled chemo-poro-thermoelastic processes on pore pressure and stress distributions around a wellbore in swelling shale. J Petrol Sci Eng 67(1):57–64

He S, Wang W, Zhou J, Huang Z, Tang M (2015) A model for analysis of wellbore stability considering the effects of weak bedding planes. J Nat Gas Sci Eng 27:1050–1062

Jaeger JC (1960) Shear failure of anistropic rocks. Geol Mag 97(1):65–72

Jaeger JC, Cook NG, Zimmerman R (2009) Fundamentals of rock mechanics. John Wiley & Sons

Jin Y, Yuan J, Hou B, Chen M, Lu Y, Li S, Zou Z (2012) Analysis of the vertical borehole stability in anisotropic rock formations. J Pet Explor Prod Technol 2(4):197–207

Lee H, Ong SH, Azeemuddin M, Goodman H (2012) A wellbore stability model for formations with anisotropic rock strengths. J Petrol Sci Eng 96:109–119

Li Y, Weijermars R (2019) Wellbore stability analysis in transverse isotropic shales with anisotropic failure criteria. J Petrol Sci Eng 176:982–993

Liang C, Chen M, Jin Y, Lu Y (2014) Wellbore stability model for shale gas reservoir considering the coupling of multi-weakness planes and porous flow. J Nat Gas Sci Eng 21:364–378

Ma T, Chen P (2015) A wellbore stability analysis model with chemical-mechanical coupling for shale gas reservoirs. J Nat Gas Sci Eng 26:72–98

Mody FK, Hale AH (1993) Borehole-stability model to couple the mechanics and chemistry of drilling-fluid/shale interactions. J Petrol Technol 45(11):1093–1101

Narayanasamy R, Barr D, Mine A (2010) Wellbore-instability predictions within the Cretaceous mudstones, Clair field, west of Shetlands. SPE Drill Complet 25(4):518–529

Speight JG (2016) 1 - Introduction to fuel flexible energy. In: Oakey J (ed) Fuel flexible energy generation. Woodhead Publishing, Boston, pp 3–27

Peška P, Zoback MD (1995) Compressive and tensile failure of inclined well bores and determination of in situ stress and rock strength. J Geophys Res Solid Earth (1987-2012) 100(B7):12791–12811

Rahman MK, Chen Z, Rahman SS (2003) Modeling time-dependent pore pressure due to capillary and chemical potential effects and resulting wellbore stability in shales. J Energy Res Technol 125(3):169–176

Tang Z, Li Q, Yin H (2018) The influence of solute concentration and temperature of drilling fluids on wellbore failure in tight formation. J Petrol Sci Eng 160:276–284

Wang Y, Li H, Mitra A, Han DH, Long T (2020) Anisotropic strength and failure behaviors of transversely isotropic shales: An experimental investigation. Interpretation 8(3):SL59–SL70

Wang Y, Papamichos E (1994) Conductive heat flow and thermally induced fluid flow around a wellbore in a poroelastic medium. Water Resour Res 30(12):3375–3384

Zhou J, He S, Tang M, Huang Z, Chen Y, Chi J, Zhu Y, Yuan P (2018) Analysis of wellbore stability considering the effects of bedding planes and anisotropic seepage during drilling horizontal wells in the laminated formation. J Petrol Sci Eng 170:507–524

Zoback MD, Barton CA, Brudy M, Castillo DA, Finkbeiner T, Grollimund BR, Moos DB, Peska P, Ward CD, Wiprut DJ (2003) Determination of stress orientation and magnitude in deep wells. Int J Rock Mech Min Sci 40(7–8):1049–1076